UDC 536.24:697.329:519.6
DOI: 10.37128/2520-6168-2025-2-1

NUMERICAL MODELING OF THERMAL PROCESSESIN VERTICAL GROUND HEAT EXCHANGERS

Vitalii YAROPUD, Doctor of Technical Sciences, Associate Professor
Vinnytsia National Agrarian University

ЯРОПУД Віталій Миколайович, д.т.н., доцент
Вінницький національний аграрний університет

The article presents the results of numerical modeling of thermal processes in vertical ground heat exchangers of concentric and U-shaped types aimed at improving the energy efficiency of microclimate control systems in agro-industrial facilities. Analytical studies of pneumatic losses demonstrated that their magnitude is nearly identical for both configurations, while the capacity of the U-shaped heat exchanger exceeds that of the concentric design by 0.9–1.7 %, confirming the feasibility of its further application. Dependencies of the U-shaped exchanger's capacity on its geometric parameters (length, diameter) and air flow rate were established, enabling optimization of its structural characteristics.

Numerical simulations conducted in Simcenter Star-CCM+ provided spatial distributions of temperature fields under various operating conditions. It was shown that, in summer, the air flow temperature decreases by 7.2 °C in the concentric and by 8.5 °C in the U-shaped exchanger, whereas in winter, the corresponding increases amount to 8.1 °C and 9.3 °C, respectively. Characteristic zones of minimum and maximum temperature values were identified at a depth of 26.75–28.50 m, which substantiates the necessity of thermal insulation within the range of 1.50–3.25 m to maintain system efficiency.

Further data processing in Wolfram Cloud enabled the derivation of second-order regression equations describing the relationships between the change in air flow temperature and effective thermal capacity with respect to inlet air temperature and air flow rate. This allowed the determination of optimal flow rates: 453.8 m³/h for the concentric and 455.2 m³/h for the U-shaped exchanger. Under these conditions, the thermal capacity of the concentric scheme ranges from 1052 to 1266 W depending on the season, while that of the U-shaped exchanger varies from 1235 to 1575 W.

The obtained results indicate that the U-shaped heat exchanger demonstrates 17–24 % higher efficiency compared to the concentric one, making it a promising solution for use in energy-efficient microclimate systems and providing a foundation for the development of adaptive control algorithms.

Key words: *vertical ground heat exchanger; concentric heat exchanger; U-shaped heat exchanger; numerical modeling; parameters; heat and mass transfer; heat capacity; energy efficiency; pneumatic losses; temperature; thermal power; microclimate systems.*

Eq. 8. Fig. 10. Table. 4. Ref. 22.

1. Problem formulation

In the conditions of Ukraine, one of the most accessible sources of low-grade heat is the soil, which at depths greater than 10 m maintains a stable temperature in the range of +9…12 °C throughout the year. Such thermal stability provides the basis for the effective operation of systems based on heat pumps. Consequently, Ukraine possesses significant potential for utilizing the energy of soil and groundwater for energy supply purposes [1, 2].

The temperature regime of the upper soil layers and bedrock is determined by the balance of solar radiation and thermal emission from the earth's surface. Solar energy is accumulated within sedimentary and crystalline rocks down to the isothermal layer, creating a natural seasonal heat reservoir. In winter, this reservoir releases stored energy, while in summer it replenishes the supply, which is particularly characteristic of groundwater saturating upper soil horizons and sedimentary deposits [3].

Thermal energy extracted from soil masses offers wide opportunities for practical application in heating, ventilation, and air conditioning systems, especially in the agricultural sector. The use of low-grade heat sources significantly reduces the demand for traditional energy carriers required to support livestock facilities, processing technologies, and product storage [4, 5].

Patent-information analysis indicates that air-based ground heat exchangers remain a relatively underexplored area. The peak of patent registrations in this field occurred between 1995 and 2000, after which activity substantially declined. At the same time, several promising technical solutions and directions for design improvement have been identified, confirming both the scientific and practical feasibility of continued research and development in this domain.

Low-grade earth heat can be harnessed for multiple purposes: building heating, domestic hot water supply, air conditioning, surface heating of walkways to prevent icing during winter, or heating of sports grounds. In international sources, such technologies are commonly referred to by the acronym GHP (geothermal heat pumps) [6, 7].

Over the past decade, there has been rapid growth worldwide in the number of systems utilizing low-grade geothermal energy for heating and air conditioning through heat pumps. These technologies are most widely implemented in the USA, Canada, Austria, Germany, Sweden, and Switzerland, with Switzerland holding a leading position in per capita utilization of low-potential geothermal energy [8].

2. Analysis of recent research and publications

The technical implementation of low-grade heat extraction from surface soil layers is carried out through heat collection systems consisting of ground heat exchangers and pipeline networks integrated with thermal engineering equipment. Depending on their design, two main types of such systems are distinguished: open-loop and closed-loop (Fig. 1).

In open-loop systems, the energy source is groundwater, which is directly supplied to the heat pump via wells. However, such systems require regular maintenance and are limited by regional geological and hydrological conditions [9, 10, 11].

Closed-loop systems involve placing heat exchangers directly into the soil mass. As the heat transfer fluid circulates through the exchanger loops, heat is extracted from the soil and transferred to the evaporator of the heat pump. When the fluid temperature exceeds that of the soil, the system can be used in reverse mode for cooling. Depending on the spatial configuration of the exchanger loops, closed-loop systems are categorized as horizontal or vertical.

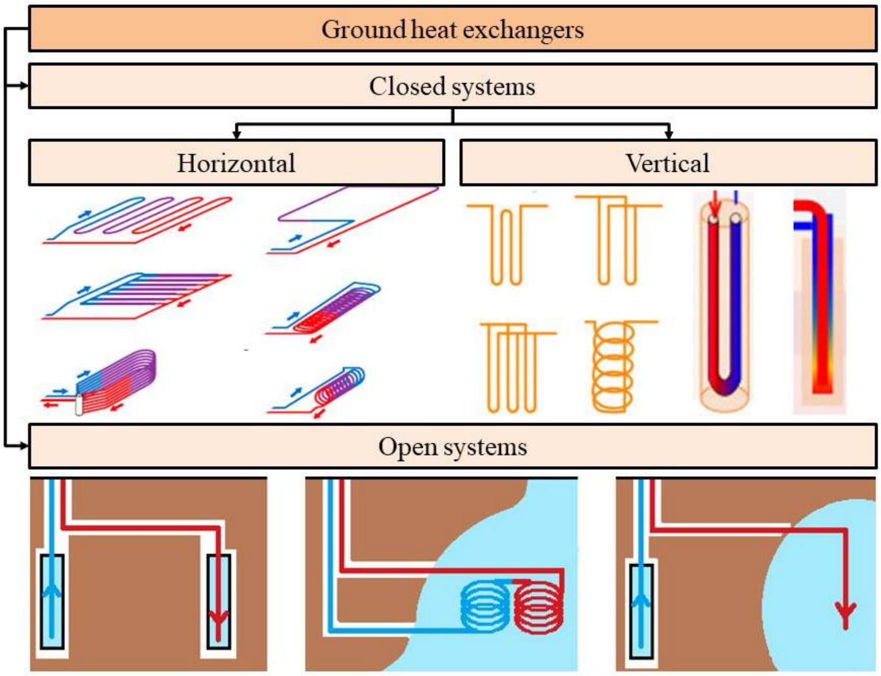

Fig. 1. Classification of ground heat exchangers [4]

Horizontal ground heat exchangers (commonly referred to in international sources as ground heat collectors *or* horizontal loops) are usually installed near buildings at shallow depths, below the level of seasonal soil freezing. Their application is limited by the available surface area, which is particularly critical in densely populated regions. In Central and Western Europe, such systems are most often constructed as individual pipelines with high density, connected either in series or in parallel. To reduce installation area requirements, alternative designs have been developed–most notably spiral heat exchangers, which can be installed in either horizontal or vertical orientations [12, 13].

Vertical ground heat exchangers (borehole heat exchangers, BHE) enable the utilization of low-grade geothermal energy at depths below the so-called «neutral zone» (10–20 m from the surface). Unlike horizontal systems, they do not require extensive land areas and are not affected by variations in solar radiation. These systems demonstrate stable performance under most geological conditions, with the exception of soils with low thermal conductivity (e.g., dry sand or gravel). Their key advantage lies in technological flexibility, allowing the creation of systems of nearly any capacity, constrained only by drilling equipment capabilities and economic feasibility.

The most widespread solution in Europe is the U-shaped exchanger, consisting of two parallel pipes connected at the bottom of the borehole. A single borehole may contain one or several pairs of pipes (typically up to three). The main advantage of this design is its relatively low manufacturing and installation cost. Another type of vertical exchanger is the coaxial (concentric) design, which consists of two pipes of different diameters arranged concentrically [14].

A comparative analysis of technical solutions demonstrates that among existing options, vertical heat exchangers ensure the highest efficiency in achieving regulatory microclimate parameters in livestock facilities. At the same time, the scientific literature still lacks sufficient research focused on determining their optimal parameters, installation conditions, and boundaries of energy feasibility. Therefore, further investigations aimed at developing recommendations for selecting rational operating modes of such systems under diverse climatic and geological conditions remain a relevant research task.

3. The purpose of the article

The aim of the study is to enhance the energy efficiency of microclimate systems through numerical modeling of thermal processes in vertical ground heat exchangers of concentric and U-shaped types.

4. Results and discussion

Based on the generalization of previous studies on the structural and technological configurations of ground air heat exchangers, two variants were selected, both characterized by relative cost-effectiveness in terms of manufacturing and operation. The first option corresponds to the results of the studies by O.S. Kovyazin and D.O. Dolhikh [15, 16, 17] and involves the use of a concentric vertical heat exchanger. For further analysis, the structural parameters determined experimentally were applied (Fig. 2a). The second option represents a classical solution-a U-shaped vertical ground heat exchanger [18] (Fig. 2b).

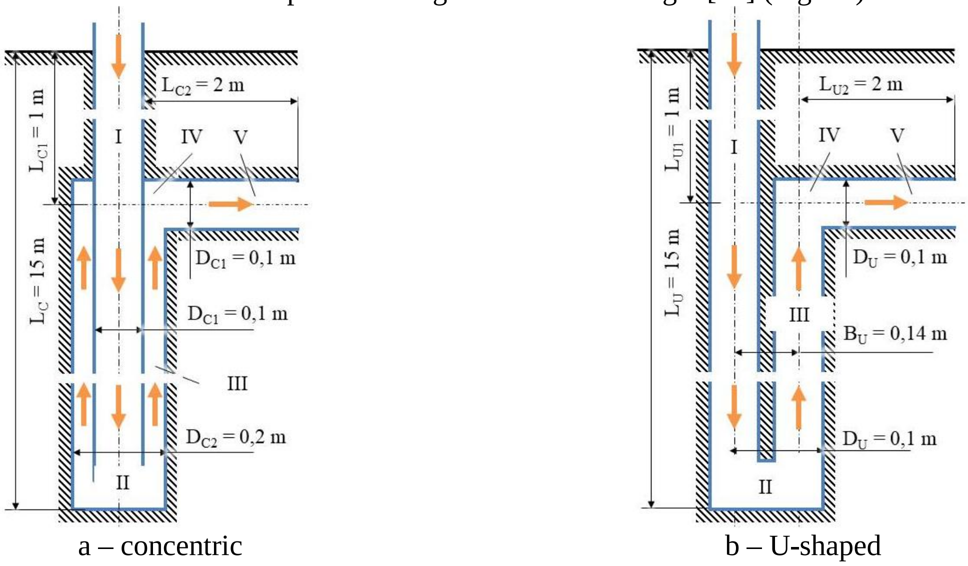

a – concentric b – U-shaped

Fig. 2. Computational scheme of vertical ground heat exchangers

According to the findings of previous research [19], where water was used as the heat transfer fluid, concentric heat exchangers demonstrate higher efficiency under short-term operation. However, during long-term use, their thermal efficiency decreases by 18–20 %. Our own experimental observations [20] also confirmed that the “pipe-in-pipe” configuration leads to secondary heat transformations through the internal walls, which adversely affect the heating or cooling processes of the airflow. Moreover, the application of thermal insulation on the inner walls results in the formation of an inactive zone that does not participate in heat exchange, while simultaneously increasing hydraulic losses.

Thus, the first stage in determining the rational configuration of a ground air heat exchanger is the assessment of the power required to drive the airflow through the system.

For a detailed analysis of the airflow, its passage through the heat exchanger should be divided into five separate sections. According to the data in [21, 22], the generalized pressure loss values for each section are presented in Table 1.

The total pressure losses in the ground air heat exchanger are determined as the sum of the pressure losses occurring in all the considered sections.

$$\Delta p_{ST} = \Delta p_{I} + \Delta p_{II} + \Delta p_{III} + \Delta p_{IV} + \Delta p_{V}. \quad (1)$$

Table 1

Pneumatic pressure losses across all sections of vertical ground heat exchangers

Section	Concentric	U-shaped
I	$\Delta p_{CI} = 0{,}11\frac{273\rho_{n.c.}\,L_C}{2TD_{C1}}\left(\frac{4q_{in}}{\pi D_{C1}^2}\right)^2 \times \left(\sqrt[4]{\frac{17\mu T\pi D_{C1}}{273q_{in}\rho_{n.c.}}+\frac{\psi}{D_{C1}}}\right)$ (2)	$\Delta p_{UI} = 0{,}11\frac{273\rho_{n.c.}\,L_U}{2TD_{U1}}\left(\frac{4q_{in}}{\pi D_{U1}^2}\right)^2 \times \left(\sqrt[4]{\frac{17\mu T\pi D_{U1}}{273q_{in}\rho_{n.c.}}+\frac{\psi}{D_{U1}}}\right)$ (7)
II	$\Delta p_{CII} = \zeta_{CII}\frac{273\rho_{n.c.}}{2T}\left(\frac{4q_{in}}{\pi D_{C1}^2}\right)^2$ (3)	$\Delta p_{UII} = 2\frac{273\alpha\rho_{n.c.}}{T}\left(\frac{4q_{in}}{\pi D_{U1}^2}\right)^2$ (8)
III	$\Delta p_{CIII} = 0{,}11\frac{273\rho_{n.c.}\left(L_C - L_{C1}\right)}{2T\sqrt{D_{C2}^2 - D_{C1}^2}}\left(\frac{4q_{in}}{\pi D_{C1}^2}\right)^2 \times \left(\sqrt[4]{\frac{17\mu T\pi D_{C1}^2}{273q_{in}\sqrt{D_{C2}^2 - D_{C1}^2}\rho_{n.c.}}+\frac{\psi}{\sqrt{D_{C2}^2 - D_{C1}^2}}}\right)$ (4)	$\Delta p_{UIII} = 0{,}11\frac{273\rho_{n.c.}\left(L_U - L_{U1}\right)}{2TD_{U1}} \times \left(\frac{4q_{in}}{\pi D_{U1}^2}\right)^2\left(\sqrt[4]{\frac{17\mu T\pi D_{U1}}{273q_{in}\rho_{n.c.}}+\frac{\psi}{D_{U1}}}\right)$ (9)
IV	$\Delta p_{CIV} = \frac{273\alpha\rho_{n.c.}}{T}\left(\frac{4q_{in}}{\pi D_{C1}^2}\right)^2$ (5)	$\Delta p_{UIV} = \frac{273\alpha\rho_{n.c.}}{T}\left(\frac{4q_{in}}{\pi D_{U1}^2}\right)^2$ (10)
V	$\Delta p_{CV} = 0{,}11\frac{273\rho_{n.c.}\,L_{C2}}{2TD_{C1}} \times \left(\frac{4q_{in}}{\pi D_{C1}^2}\right)^2\left(\sqrt[4]{\frac{17\pi D_{C1}\mu T}{273q_{in}\rho_{n.c.}}+\frac{\psi}{D_{C1}}}\right)$ (6)	$\Delta p_{UV} = 0{,}11\frac{273\rho_{n.c.}\,L_{U2}}{2TD_{U1}} \times \left(\frac{4q_{in}}{\pi D_{U1}^2}\right)^2\left(\sqrt[4]{\frac{17\pi D_{U1}\mu T}{273q_{in}\rho_{n.c.}}+\frac{\psi}{D_{U1}}}\right)$ (11)

where $\rho_{n.c.}$ = 1,293 kg/m³ – air density under normal conditions [21]; L – length of the air duct, m; T – air flow temperature, K; 273 – temperature corresponding to 0 °C, K; D – diameter of the air duct, m; q_{in} – inlet air flow rate, m³/s; μ = 18,27·10^{-6} N·s/m² – dynamic viscosity of air; ψ = 0,1 mm (for polyethylene) – equivalent roughness of the air duct walls; ζ = 2 – local resistance coefficient for a spatial (annular) 180° bend under pressure; α = 0,55 – impact reduction coefficient (for a bend of constant cross-section).

The power required to ensure the airflow through the vertical ground heat exchanger is determined using the following calculation relationship:

$$N_{ST} = \frac{q_{in}\,\Delta p_{ST}}{\eta_{п}}, \quad (2)$$

where $\eta_{п}$ – overall efficiency of the fan, $\eta_{п}$ = 0,8 [21].

Based on a comprehensive calculation of dependencies (2)–(11) performed in the Wolfram Cloud environment, functional relationships were obtained for the variation of the consumed power (N_{ST}) of the U- shaped vertical ground heat exchanger. A correlation was established between the consumed power and the main structural parameters of the exchanger–its length (L_{U1}), diameter (D_{U1}), and air flow rate (q_{in}). The corresponding graphical dependencies are presented in Fig. 3.

A comparative analysis of the calculated power values showed that, for the U-shaped vertical ground heat exchanger, the value exceeds that of the concentric design by 0.9–1.7%. This indicates an almost identical level of pressure losses in both structural configurations. Therefore, further evaluation of their efficiency should be based on the investigation of the thermal capacity of the heat exchangers.

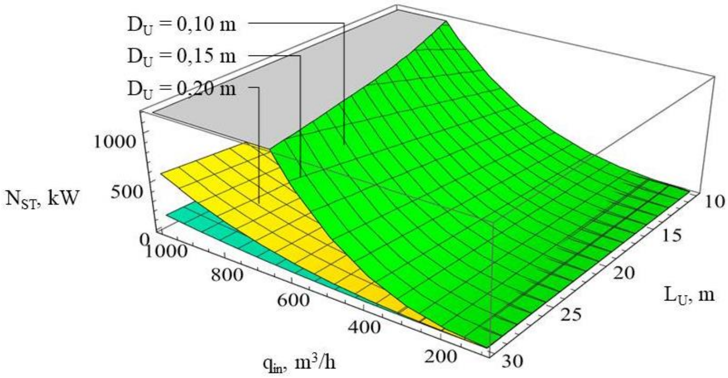

Fig. 3. Dependencies of the power variation (N_{ST}) of the U-shaped vertical ground heat exchanger on its length (L_{U1}), diameter (D_{U1}), and air flow rate (q_{in})

Numerical modeling was carried out using the Simcenter Star-CCM+ software package, which applies spatial discretization based on the finite volume method with the determination of unknown variables at the centers of control cells. To reduce the number of mesh elements and optimize computational resource consumption, a symmetry condition relative to the XOZ plane was applied. The general view of the generated computational mesh and the structural and technological characteristics of the two variants of vertical ground heat exchangers are presented in Fig. 4.

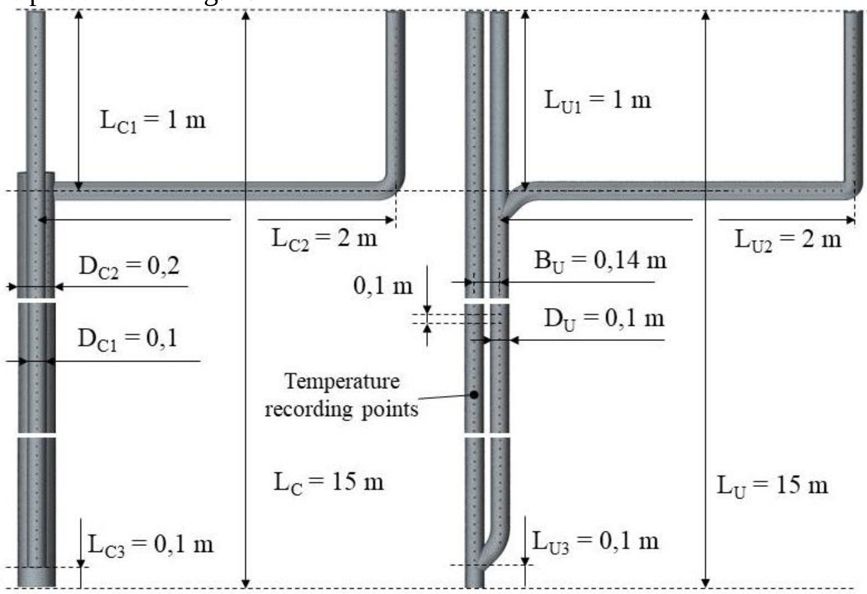

a b

Fig. 4. General view of the generated computational mesh and the structural-technological parameters of the concentric (a) and U-shaped (b) vertical ground heat exchangers

In constructing the physical models of airflow, the following approaches were applied: three-dimensional modeling, Eulerian multiphase model, segregated flow method and Volume of Fluid (VOF) model, phase interaction model, as well as the approach using separate multiphase temperatures. The flow dynamics were described by the Navier–Stokes equations with the application of the k–ε turbulence model.

Air and water were considered as Eulerian phases. The air phase was represented using the real gas model MASVP-PR97 (water vapor) with consideration of turbulence characteristics, while the water phase was modeled with the Van der Waals real gas model, also accounting for turbulence.

Physical modeling of the walls of the ventilation system supplying clean air was carried out using a three-dimensional solid description approach, assuming constant density and applying the separate solid energy model.

For constructing the physical models of the soil medium, the following approaches were employed: three-dimensional solid modeling, the assumption of constant density, and the application of the separate solid energy model.

The physico-mechanical characteristics of all phases involved in the modeling are summarized in Table 2.

Table 2

Physico-mechanical properties of soil

Parameter	Ground
Thermal conductivity coefficient, W/(m·K)	0,46
Specific heat capacity, J/(kg·K)	1590,0

An unsteady implicit solver with 10 inner iterations was applied for the calculations. The total simulation time amounted to 105 s.

As a result of the computations, the spatial distribution of the temperature field in the vertical ground heat exchangers was obtained for summer operating conditions (Fig. 5).

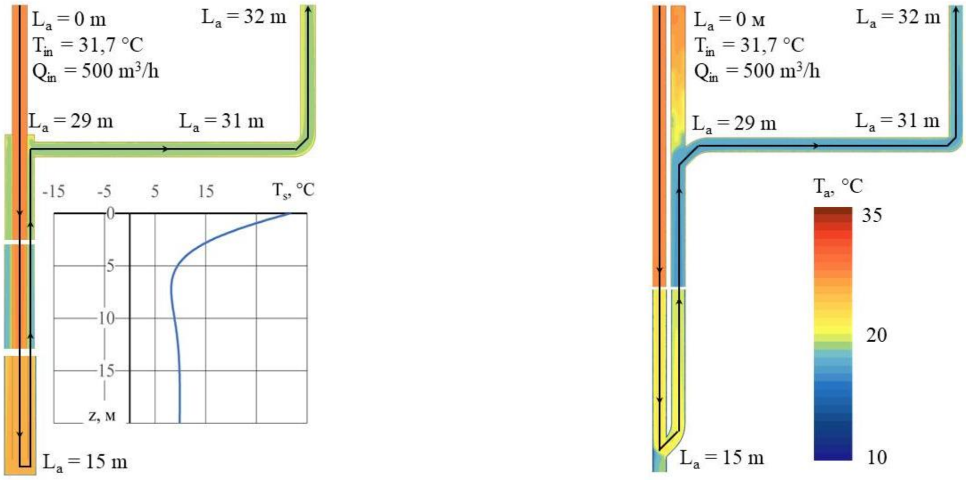

a ***b***

Fig. 5. Temperature field distribution of the concentric (a) and U-shaped (b) vertical ground heat exchangers during the summer period at an air supply rate of 500 m³/h.

For a more detailed representation of the numerical simulation results, a graphical dependence of the air flow temperature (T_a) on the length of its flow path (L_a) was constructed. The obtained result is presented in Fig. 6.

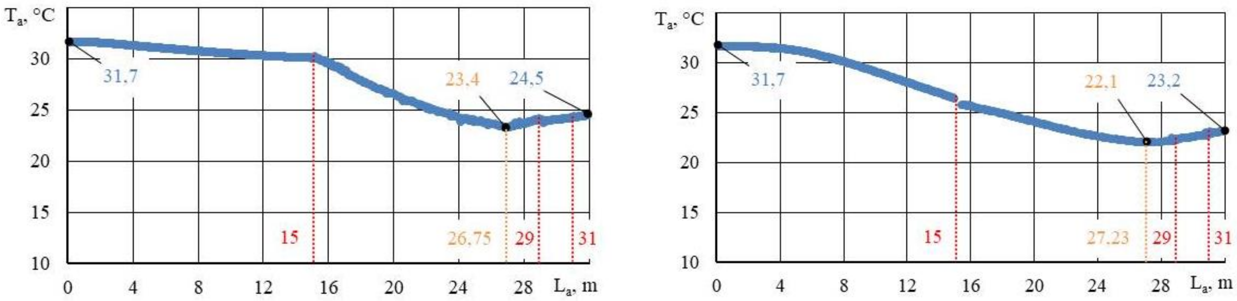

a ***b***

Fig. 6. Graph of the dependence of air flow temperature (T_a) on the flow path length (L_a) for the concentric (a) and U-shaped (b) vertical ground heat exchangers during the summer period at an air supply rate of 500 m³/h

Analysis of the results presented in Figs. 5–6 shows that, during the summer period, the air flow temperature along a pipeline with a total length of 32 m decreases from 31.7 °C to 24.5 °C in the case of the concentric heat exchanger and to 23.2 °C in the case of the U-shaped exchanger. Thus, the largest temperature drop is observed for the U-shaped configuration, amounting to 8.5 °C, which exceeds the corresponding value of the concentric heat exchanger (7.2 °C).

According to the graphs in Fig. 6, the minimum temperature values are reached at a distance of 26.75 m for the concentric exchanger (23.4 °C) and at 27.23 m for the U-shaped exchanger (22.1 °C). It was established that applying thermal insulation to the air duct to a depth of no less than 3.25 m makes it possible to preserve the minimum air flow temperature until the point of exit from the exchanger.

Further analysis was conducted for winter conditions. The distribution of temperature fields and the corresponding graphical dependencies are presented in Figs. 7–8.

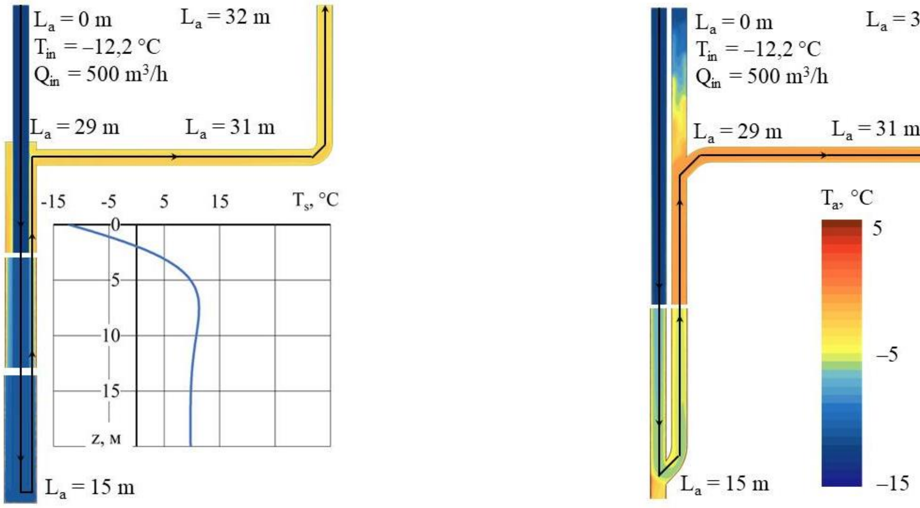

a ***b***

Fig. 7. Temperature field distribution of the concentric (a) and U-shaped (b) vertical ground heat exchangers during the winter period at an air supply rate of 500 m³/h

According to the results presented in Figs. 7–8, during the winter period the air flow temperature along a 32 m pipeline increases from –12.2 °C to –4.1 °C in the case of the concentric heat exchanger and to –2.9 °C for the U-shaped exchanger. The U-shaped configuration provides the greatest temperature rise (9.3 °C), which exceeds the corresponding value of the concentric exchanger (8.1 °C).

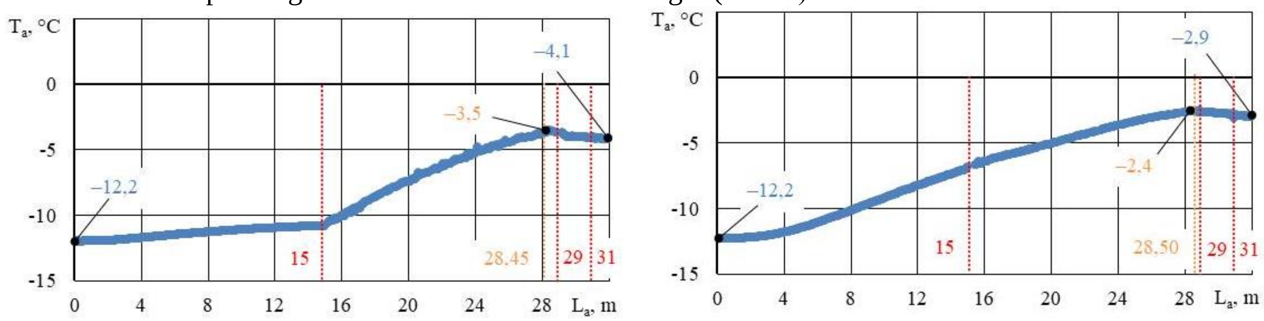

a ***b***

Fig. 8. Graph of the dependence of air flow temperature (T_a) on the flow path length (L_a) for the concentric (a) and U-shaped (b) vertical ground heat exchangers during the winter period at an air supply rate of 500 m³/h

An analysis of the graphs (Fig. 8) shows that the maximum air flow temperatures are observed at a distance of 28.45 m for the concentric scheme (–3.5 °C) and 28.50 m for the U-shaped scheme (–2.4 °C). The obtained results confirm the feasibility of applying thermal insulation to the air duct at depths of no less than 3.25 m.

In subsequent numerical experiments, the air duct insulation was assumed within the depth range of 1.50–2.77 m, taking into account the minimum outlet air temperatures of the heat exchanger.

To substantiate the rational operating parameters, their variation was carried out within the following ranges:

– inlet air temperature T_{in}: –12.2 °C; –1.225 °C; 9.75 °C; 20.725 °C; 31.7 °C;

– air flow rate Q_{in}: 200; 350; 500; 650; 800 m³/h.

Based on the results of numerical modeling performed in the Simcenter Star-CCM+ environment and subsequent data processing in Wolfram Cloud, a second-order regression equation was obtained, which describes the dependence of the air flow temperature change (ΔT_a) on the studied factors in coded form for each heat exchanger variant:

– concentric heat exchanger

$$\Delta T_{aC} = 0{,}694578 - 0{,}175916\, X_1 + 7{,}80171\, X_1^2 - 2{,}16185\, X_2 + 0{,}296869\, X_1 X_2 + 0{,}193303\, X_2^2; \tag{3}$$

– U-shaped heat exchanger

$$\Delta T_{aU} = 1{,}13879 - 0{,}354688\, X_1 + 8{,}84877\, X_1^2 - 2{,}55882\, X_2 + \tag{4}$$

$+ 0{,}692671\ X_1 X_2 + 0{,}184519\ X_2^2.$

The statistical processing of equations (3) and (4) is presented in Tables 3–4.

Table 3

Results of the statistical processing of equation (13)

Coefficient	Value	Error	Student's t-test	Probability
a_{00}	0,694578	0,166418	4,17369	0,000515338
a_{10}	–0,175916	0,119835	–1,46799	0,158468
a_{20}	–2,16185	0,119835	–18,0403	$2{,}05781 \cdot 10^{-13}$
a_{12}	0,296869	0,169472	1,75173	0,0959463
a_{11}	7,80171	0,202558	38,516	$1{,}68977 \cdot 10^{-19}$
a_{22}	0,193303	0,202558	0,954309	0,351912

Table 4

Results of the statistical processing of equation (14)

Coefficient	Value	Error	Student's t-test	Probability
a_{00}	1,13879	0,182225	6,24936	$5{,}30966 \cdot 10^{-6}$
a_{10}	–0,354688	0,131217	–2,70306	0,0140958
a_{20}	–2,55882	0,131217	–19,5007	$5{,}04048 \cdot 10^{-14}$
a_{12}	0,692671	0,185569	3,73268	0,00141061
a_{11}	8,84877	0,221798	39,8957	$8{,}72541 \cdot 10^{-20}$
a_{22}	0,184519	0,221798	0,831927	0,415784

Comparison of the calculated Student's t-test values with the tabular value $t_{0.05(25)} = 2.06$ made it possible to eliminate statistically insignificant coefficients of the regression equations. Based on this analysis, equations (3) and (4) are presented in decoded form as follows:

– concentric heat exchanger

$$\Delta T_{aC} = 5{,}915 - 0{,}00721\ Q_{in} - 0{,}3238\ T_{in} + 0{,}0162\ T_{in}^2; \quad (5)$$

– U-shaped heat exchanger

$$\Delta T_{aU} = 7{,}819 - 0{,}00956\ Q_{in} - 0{,}4269\ T_{in} + 0{,}0001052\ Q_{in}\ T_{in} + 0{,}01837\ T_{in}^2. \quad (6)$$

The graphical interpretation of dependencies (5) and (6) is presented in Fig. 9.

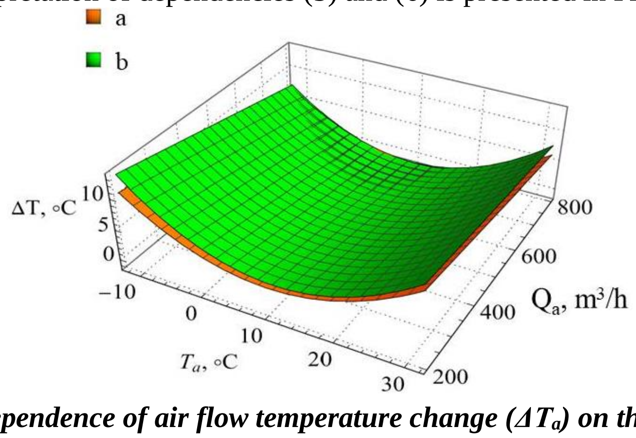

Fig. 9. Graphs of the dependence of air flow temperature change (ΔT_a) on the studied factors for the concentric (a) and U-shaped (b) vertical ground heat exchangers.

Figure 9 shows the dependencies of the air flow temperature change (ΔT_a) on the inlet air temperature (T_{in}) and air flow rate (Q_{in}) for concentric and U-shaped vertical ground heat exchangers. As can be seen from the graphs, higher values of ΔT_a are characteristic of the U-shaped configuration. With an increase in air flow rate (Q_{in}), a decrease in the temperature difference is observed. The maximum values of ΔT_a were recorded under conditions of high (summer period, T_{in} = 31.7 °C) and low (winter period, T_{in} = −12.2 °C) inlet air temperatures. In contrast, for T_{in} = 9.6 °C, the minimum value of ΔT_a was obtained, which corresponds to the physical picture of the process, since the soil temperature at a depth of more than 12.3 m is T_m = 9.79 °C (Fig. 8).

Statistical analysis of equations (5) and (6) within the studied variation range confirmed their reliability: the Pearson correlation coefficient was 0.94, and the Fisher criterion $F = 2.12 < F_t = 2.49$. This indicates the adequacy of the obtained mathematical model.

As the airflow moves through the ground heat exchanger, interaction with the air duct walls occurs, causing pneumatic losses. In this regard, the effective thermal capacity of the ground heat exchanger was chosen as the optimization criterion, which is calculated according to the following dependency:

$$N_E = N_T - N_{ST}, \tag{7}$$

where N_T – thermal capacity of the ground heat exchanger, W; N_{ST} – power required to drive the airflow through the ground heat exchanger, W.

Thermal capacity of the ground heat exchanger:

$$N_T = \frac{Q_{in}}{3600} \rho_a (T_{in}) c_a \Delta T_a, \tag{8}$$

where Q_{in} – volumetric air flow rate, m³/h; $\rho_a(T_{in}) = \frac{273}{273 + T_{in}} \rho_{н.у.}$ – air density at the outlet of the heat exchanger, kg/m³; c_a – specific heat capacity of air, taken as c_a = 1003.62 J/(kg·°C); ΔT_a – temperature difference between the inlet and outlet of the heat exchanger, °C.

By combining equations (7), (8), (5) or (6), as well as (2), (1), generalized dependencies of the effective thermal capacity of ground heat exchangers (N_E) on the inlet air temperature (T_{in}) and air flow rate (Q_{in}) were obtained using the Wolfram Cloud environment. The corresponding graphical results are presented in Fig. 10.

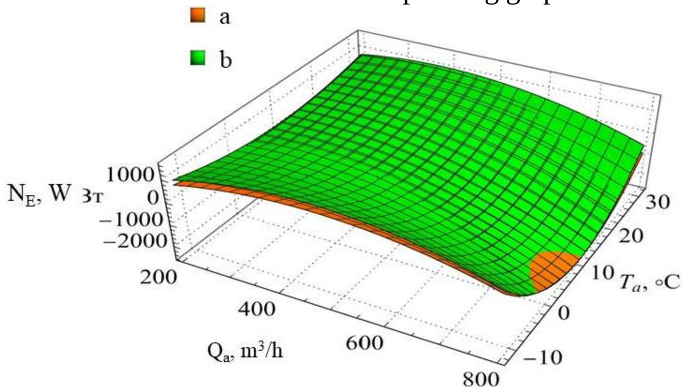

Fig. 10. Graphs of the effective thermal capacity N_E versus the study factors for the concentric (a) and U-shaped (b) vertical ground heat exchangers.

Taking into account the condition of maximizing the effective thermal capacity of ground heat exchangers (N_{EN}), the rational air flow rates were determined as Q_{in} = 453.8 m³/h for the concentric configuration and Q_{in} = 455.2 m³/h for the U-shaped configuration. Under these conditions, the effective thermal capacity of the concentric heat exchanger is:

$$N_{EC}(T_{in} = 31{,}7\ °C) = 1266\ W,\ N_{EC}(T_{in} = -12{,}2\ °C) = 1052\ W,$$

which is lower than the corresponding values for the U-shaped design:

$$N_{EU}(T_{in} = 31{,}7\ °C) = 1575\ W,\ N_{EU}(T_{in} = -12{,}2\ °C) = 1235\ W.$$

Thus, the U-shaped vertical ground heat exchanger was found to be 17–24% more efficient than the concentric one. It was also established that the minimum temperature difference between the air and the ground, at which the effective thermal capacity of the exchanger remains positive (N_{EU}>0), is ΔT_G = 9.3°C.

5. Conclusion

Analytical studies of pneumatic losses in vertical ground heat exchangers for the two proposed configurations (concentric and U-shaped) showed that the capacity of the U-shaped exchanger exceeds that of the concentric design by 0.9–1.7 %. This suggests that the level of pneumatic losses in both constructions is nearly identical. In addition, the dependence of the power output N_{ST} of the U-shaped exchanger on its length L_{U1}, diameter D_{U1}, and air flow rate qin was established (Fig. 3).

Numerical simulations of heat transfer processes performed *in* Simcenter Star-CCM+ made it possible to obtain the spatial distribution of the temperature field for both exchanger variants under summer and winter operating conditions. It was found that, in summer, the air flow temperature decreases by 7.2 °C in the concentric exchanger and by 8.5 °C in the U-shaped one. In winter, the corresponding increases amount to 8.1 °C and 9.3 °C, respectively. The lowest (summer) and highest (winter) air temperature values were recorded at pipeline sections 26.75–28.50 m in length. This confirmed the necessity of applying thermal insulation within the depth range of 1.50–3.25 m to preserve minimal temperature values until the air exits the exchanger.

Further processing of the simulation results in Wolfram Cloud made it possible to derive second-order regression equations describing the dependencies of the air temperature change (ΔT_a) and effective thermal capacity (N_E) on the inlet air temperature (T_{in}) and air flow rate (Q_{in}) for each exchanger configuration.

Considering the condition of maximizing effective thermal capacity, rational air flow rates were determined: Q_{in}=453.8 m³/h for the concentric exchanger and Q_{in} = 455.2 m³/h for the U-shaped exchanger. Under these conditions, the effective thermal capacity of the concentric design is $N_{EC}(T_{in} = 31.7°C) = 1266$ W and $N_{EC}(T_{in} = –12.2°C) = 1052$ W, which is lower than the corresponding values for the U-shaped exchanger: $N_{EU}(T_{in} = 31.7°C) = 1575$ W and $N_{EU}(T_{in} = –12.2°C) = 1235$ W.

Thus, the U-shaped vertical ground heat exchanger demonstrates 17–24% higher efficiency compared to the concentric configuration, confirming its feasibility for application in energy-efficient microclimate systems.

References

1. Kaletnik, G.M. (2008). Energy supply of Ukraine and possibilities of using potential sources of renewable energy. *Visnyk agrarnoyi nauky, 10,* 50–55. [in Ukrainian].
2. Dolhikh, D.O. (2012). Analysis and classification of ground heat exchangers. *Mechanization, ecologization and conversion of bio-raw materials in animal husbandry: Proceedings of the Institute of Mechanization of Animal Husbandry NAAS, 1(9),* 56–63. [in Ukrainian].
3. Blázquez, C.S., Bruno, J.C., Rigola, J. and Coronas, A. (2023). Multiparametric evaluation of electrical, biogas and natural gas geothermal source heat pumps. In *Geothermal Heat Pump Systems*. Cham: Springer, 103–122. DOI: 10.1007/978-3-031-24524-4_4. [in English].
4. Dolhikh, D.O. (2017) *Substantiation of structural and technological parameters of a ground heat exchanger for ventilation of livestock premises*. PhD thesis. National University of Life and Environmental Sciences of Ukraine. [in Ukrainian].
5. Kaletnik, H.M., Yaropud, V.M. (2022). Results of numerical simulation of geothermal cooling in the ventilation system of livestock premises. *Vibrations in engineering and technology, 3(106),* 5–12. DOI: 10.37128/2306-8744-2022-3-1. [in Ukrainian].
6. Almutairi, K. (2022). Applications of intelligent techniques in modeling geothermal heat pumps: an updated review. *International Journal of Low-Carbon Technologies, 17,* 910–918. DOI: 10.1093/ijlct/ctac061. [in English]
7. Karami, M., Delfani, S. and Esmaeelian, J. (2022). Recent progress in geothermal heat pumps. in *Recent Advances in Renewable Energy Technologies.* Elsevier, 287–320. DOI: 10.1016/B978-0-12-823532-4.00001-X. [in English].
8. Hou, G., Liu, Z., Zhao, M., Taherian, H., Jiang, W. and Chen, D. (2021). Underground energy: utilization of geothermal shallow heat pumps. in Jeguirim, M. (ed.) *Recent Advances in Renewable Energy Technologies*. Academic Press, 211–247. DOI: 10.1016/B978-0-323-91093-4.00002-0. [in English].
9. Halilovic, S., García Gil, A., Vázquez-Suñé, E., Carrera, J. (2023). Optimization approaches for the design and operation of open-loop shallow geothermal systems. *Advances in Geosciences, 62,* 57–66. DOI: 10.5194/adgeo-62-57-2023. [in English].
10. Kaletnik, H., Yaropud, V., Lutkovska, S., Aliiev, E. (2024). Studying the air flow heating process in the vertical type ground heat exchanger. *Przeglad Elektrotechniczny, 100(10),* 46–54. DOI: 10.15199/48.2024.10.08. [in English].
11. Kaletnik, G., Yaropud, V. and Babyn, I. (2024) *Development of resource-saving technical and technological support for production and animal husbandry*. Boston, USA: Primedia. DOI: 10.46299/979-8-89619-784-3. [in English].
12. Kayaci, N. and Demir, H. (2018). Numerical modelling of transient soil temperature distribution for horizontal ground heat exchanger of ground source heat pump. *Geothermics, 73,* 33–47. DOI: 10.1016/j.geothermics.2018.01.009. [in English].
13. Tang, F., Li, Y., Wang, L., Zhao, J. and Guo, Y. (2021). A numerical study into effects of soil compaction and heat storage on thermal performance of a horizontal ground heat exchanger. *Renewable Energy, 172,* 740–752. DOI: 10.1016/j.renene.2021.03.025. [in English].
14. Hałaj, E., Pająk, L. and Papiernik, B. (2020). Finite element modeling of geothermal source of heat pump in long-term operation. *Energies, 13(6),* 1341. DOI: 10.3390/en1306134. [in English].
15. Kovyazin, O.S. and Dolhikh, D.O. (2013). Substantiation of the construction of a ground heat exchanger. *Bulletin of Kharkiv Petro Vasylenko National Technical University of Agriculture, 132,* 167–170. [in Ukrainian].
16. Kovyazin, O.S. (2018). Substantiation of the diameter of the casing pipe of the ground heat exchanger and the air supply into it. *Bulletin of the National Technical University «KhPI». Series: Power and Heat Engineering*

Processes and Equipment, 12(1288), 71–74. DOI: 10.20998/2078-774X.2018.12.13. [in Ukrainian].
17. Yaropud, V.M. (2024). Study of the efficiency of functioning of the mechatronic system for ensuring the microclimate of livestock premises. *Engineering, Energy, Transport of AIC, 1(124),* 56–72. DOI: 10.37128/2520-6168-2024-1-7. [in English].
18. Sydorchuk, B., Naumchuk, O. and Mazurek, P. (2021). Modeling of joint operation of a ground soil heat exchanger and a thermal pump evaporator. *Journal of Ecological Engineering, 22(2),* 256–261. DOI: 10.12911/22998993/131177. [in Ukrainian].
19. Jalaluddin, J., Akio, M., Koutaro, T. and Kentaro, Y. (2010). Thermal performances of three types of ground heat exchangers in short-time period of operation. *International Refrigeration and Air Conditioning Conference*. 1123. URL: http://docs.lib.purdue.edu/iracc/1123. [in English].
20. Yaropud, V.M. (2016) *Substantiation of design and operating parameters of a heat recuperator for livestock premises*. PhD thesis. Vinnytsia National Agrarian University. [in Ukrainian].
21. Zhukovskyi, S.S. (2003) *Aerodynamics of ventilation.* Lviv: Lviv Polytechnic National University. [in Ukrainian].
22. Kupchuk, I.M., Yaropud, V.M., Telekalo, N.V. and Hranyak, V.F. (2020). Prospects and prerequisites for the introduction of autonomous power supply systems of agro-industrial enterprises. *Engineering, Energy, Transport of AIC, 3(110),* 51–63. DOI: 10.37128/2520-6168-2020-3-5. [in Ukrainian].

ЧИСЕЛЬНЕ МОДЕЛЮВАННЯ ТЕПЛОВИХ ПРОЦЕСІВ У ВЕРТИКАЛЬНИХ ҐРУНТОВИХ ТЕПЛООБМІННИКАХ

У статті представлено результати чисельного моделювання теплових процесів у вертикальних ґрунтових теплообмінниках концентричного та U-подібного типів з метою підвищення енергоефективності систем мікроклімату приміщень агропромислового комплексу. Проведені аналітичні дослідження пневмовтрат показали, що їх величина для обох конструкцій є майже однаковою, а потужність U-подібного теплообмінника перевищує показник концентричного на 0,9–1,7 %, що підтверджує доцільність його подальшого використання. Встановлено залежності потужності U-подібного теплообмінника від його геометричних параметрів (довжини, діаметра) та витрати повітря, що дозволяє оптимізувати конструктивні характеристики.

Чисельне моделювання у середовищі Simcenter Star-CCM+ дало змогу отримати просторові розподіли температурних полів у різних режимах експлуатації. Показано, що в літній період температура повітряного потоку зменшується на 7,2 °С у концентричному та на 8,5 °С у U- подібному теплообміннику, тоді як у зимовий період відбувається зростання відповідно на 8,1 та 9,3 °С. Визначено характерні зони мінімальних і максимальних значень температури на глибині 26,75– 28,50 м, що обґрунтовує необхідність теплоізоляції ділянки 1,50–3,25 м для збереження ефективності роботи системи.

Подальша обробка даних у Wolfram Cloud дала можливість отримати рівняння регресії другого порядку, які описують залежності зміни температури повітряного потоку та ефективної теплової потужності від початкової температури та витрати повітря. Це дозволило визначити оптимальні значення витрат: 453,8 м³/год для концентричного та 455,2 м³/год для U-подібного теплообмінника. За цих умов теплова потужність концентричної схеми становить 1052–1266 Вт в залежності від сезону, тоді як для U-подібного – 1235–1575 Вт.

Отримані результати свідчать, що U-подібний теплообмінник забезпечує на 17–24 % вищу ефективність порівняно з концентричним, що робить його перспективним рішенням для використання в енергоефективних системах мікроклімату та дає підґрунтя для розробки адаптивних алгоритмів їх керування.

Ключові слова: *вертикальний ґрунтовий теплообмінник, концентричний теплообмінник, U-подібний теплообмінник, чисельне моделювання, параметри, тепло і масообмін, теплоємність, енергоефективність, пневмовтрати, температура, теплова потужність, системи мікроклімату.*

Ф. 8. Рис. 10. Табл. 4. Літ. 22.

INFORMATION ABOUT THE AUTHORS

Vitalii YAROPUD – Doctor of Technical Sciences, Associate Professor of the department of machinery and equipment for agricultural production, Vinnytsia National Agrarian University (St. Soniachna, 3, Vinnytsia, Ukraine, 21008, e-mail: yaropud77@gmail.com, https://orcid.org/0000-0003-0502-1356).

ЯРОПУД Віталій Миколайович – доктор технічних наук, доцент кафедри машин та обладнання сільськогосподарського виробництва Вінницького національного аграрного університету (вул. Сонячна, 3, м. Вінниця, Україна, 21008, e-mail: yaropud77@gmail.com, https://orcid.org/0000-0003-0502-1356).